ELSEVIER

Polymer 43 (2002) 3441–3446

polymer

www.elsevier.com/locate/polymer

Microscopic lamellar organization in high-density polyethylene banded spherulites studied by scanning probe microscopy

S. Sasaki[a,*], Y. Sakaki[a], A. Takahara[b], T. Kajiyama[a]

[a]*Department of Applied Chemistry, Graduate School of Engineering, Kyushu University, 6-10-1 Hakozaki, Higashi-ku, Fukuoka 812-8581, Japan*
[b]*Institute for Fundamental Research of Organic Chemistry, Kyushu University, 6-10-1 Hakozaki, Higashi-ku, Fukuoka 812-8581, Japan*

Dedicated to Professor Imanishi on the occasion of his retirement

Received 17 January 2002; received in revised form 21 February 2002; accepted 22 February 2002

Abstract

Surface topography and lamellar aggregation structure of high-density polyethylene (HDPE) banded spherulites were investigated by scanning probe microscopy. HDPE films were prepared by isothermal crystallization at various crystallization temperatures from the melt. Polarizing near-field scanning optical microscopic (NSOM) observations for the HDPE films revealed submicron-scale correlation between surface topography and birefringence of banded spherulites. The height profile of the film surface along the spherulitic radius periodically changed corresponding to the intensity profile of transmitted light along the radius of the extinction ring. This correlation was more clearly observed in the topographic and NSOM images of permanganic etched PE films. Therefore, it was apparently suggested that the crystallographic *c*-axis of the orthorhombic unit cell was parallel and perpendicular to the film surface at the peak and the valley in the surface corrugation of the banded spherulite, respectively. The band spacing obtained by polarizing NSOM and atomic force microscopy (AFM) was comparable to that determined by polarizing far-field optical microscopic observation under crossed nicols. The band spacing and the peak-to-valley height difference in the corrugation increased with an increase in isothermal crystallization temperature. AFM observations directly indicated local lamellar orientation and stacking manner. © 2002 Elsevier Science Ltd. All rights reserved.

Keywords: HDPE banded spherulite; Atomic force microscopy; Polarizing near-field scanning optical microscopy

1. Introduction

Polyethylene (PE) spherulites have been studied as the standard examples on the structure of semi-crystalline polymers, by polarizing optical microscopy (POM) [1–8], transmission electron microscopy (TEM) [9–14] and X-ray diffraction [15]. The banded spherulite of PE is generally characterized by the extinction ring in POM, which reflects a periodic arrangement of birefringent units along the spherulitic radii. In the dark part of the extinction ring in the POM image resulted from the zero-amplitude effects, the crystallographic *ab* plane is perpendicular to the incident light. In the bright part, on the other hand, the crystallographic *bc* plane is nearly perpendicular to it. The crystallographic *b*-axis of the orthorhombic unit cell is namely parallel to the spherulitic radius and the crystallographic *a*- and *c*-axes rotate around it. This concerted twisting of crystallographic orientation about the spherulitic radius, so-called banding, relates to lamellar twisting. Keith and Padden Jr. explained the banding in PE spherulites based on smooth twisting of leading lamellae near their growth tips [4,7]. On the other hand, Bassett et al. proposed quasidiscontinuous twisting of relatively planar lamellae [9,13]. However, there is still no general agreement about how and why crystalline lamellae twist in the spherulites.

The banding structure of PE spherulites was influenced by crystallization condition. TEM observations indicate morphological difference in fibrous textures of the banded spherulites crystallized at various temperatures from the melt [11]. Lamellar twisting manner changes depending on the crystallization temperature, which reflects the band spacing of the extinction ring in POM [16]. However, how the crystallization temperature influences local lamellar organization has not been revealed in detail.

In the case of TEM studies, radiation damage to samples is generally occurred. Therefore, it is reasonable to consider that textural feature of samples might be partly changed by electrons. Atomic force microscopy (AFM) overcomes this problem by direct visualization of samples without any surface treatment. Also, polarizing near-field scanning optical microscopy (NSOM) is able to obtain birefringence

---

* Corresponding author. Tel./fax: +81-92-642-3560.
E-mail address: s.sasaki@cstf.kyushu-u.ac.jp (S. Sasaki).

0032-3861/02/$ - see front matter
PII: S0032-3861(02)00158-1

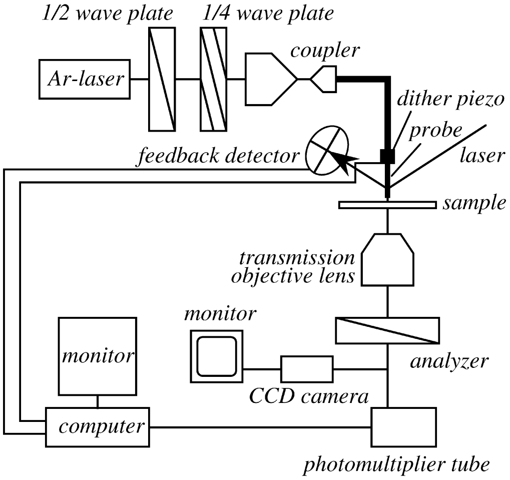

Fig. 1. Schematic representation of the polarizing NSOM system used in this study.

properties of samples in submicron scale. From these points of views, AFM and polarizing NSOM are effective and promising methods to reveal lamellar aggregation structure of the banded spherulites.

The purpose of this study is to clarify the structural and morphological features of HDPE banded spherulites in lamellar resolution scale by polarizing NSOM and AFM. AFM height profiles were compared with NSOM light intensity profiles of the extinction ring to reveal the relationship between surface topography and local lamellar orientation of the banded spherulites. The crystallization temperature dependences of surface topography and local birefringence of the banded spherulites were also investigated in the order of micrometer down to nanometer scales.

2. Experimental section

2.1. Samples

HDPE (Marlex 9) with the weight average molecular weight, M_w, of 520 k and large molecular weight distribution was used as a sample. A 0.5 w/w% *p*-xylene solution of HDPE was cast onto a coverslip kept at 423 K, and then, the solvent was quickly evaporated from the solution. The obtained HDPE film on the coverslip was melted at 423 K for 1 h under N_2 gas flow. Afterwards, the film was isothermally crystallized at various crystallization temperatures, T_c, under N_2 gas flow. Thickness of the crystallized films was ca. 3 μm.

In order to reveal internal lamellar aggregation structure of HDPE spherulites, the surface of HDPE films was etched with permanganic reagent, a 0.8w/v% solution of potassium permanganate in concentrated sulfuric acid [10]. The HDPE film on the coverslip was immersed in the etching reagent at 293 K for 1.5 min. Etched films were washed with a dilute solution of sulfuric acid, a solution of hydrogen peroxide, pure water and acetone using an ultrasonic bath [12].

2.2. Experiments

The surface morphology of HDPE films was observed by AFM. AFM images were obtained with a SPA300 (Seiko Instrument Industry Co., Ltd) under the contact mode operation at ca. 303 K in air. The cantilever used in this study was a rectangular-shaped one with a quadrangular pyramid of Si_3N_4 microtip. The bending spring constant of the cantilever was 0.09 N/m.

The birefringence of the HDPE banded spherulites was investigated by polarizing NSOM. Polarizing NSOM images were obtained for the films with an Aurora (Thermo Microscopes, Inc.). Fig. 1 shows a schematic representation of the polarizing NSOM system. An Ar laser (488 nm) utilized as the near-field light source was passed through a $\lambda/4$ wave plate and a $\lambda/2$ wave plate to control the polarization before being coupled into an optical fiber probe. The light emitted by the near-field aperture of the probe was transmitted through a sample via the analyzer to a photomultiplier tube. The aperture system acted as a $\lambda/4$ wave plate. The extinction ratio in this setup without sample was 11–20. NSOM overcomes the resolution limited by the diffraction at the aperture in conventional or far-field optical microscopy, and then, optical imaging is realized with submicrometer resolution. Since the resolution of the images is determined mainly by the wavelength of light source and its near-field distance to the sample, the shear force probe feedback system was utilized to control the distance between the probe and the sample surface with nanometers during scanning. In practical, optical and topographic images were obtained simultaneously in our study. POM observation was also performed for HDPE films with an OPTIPHOT2-POL (Nikon, Co.) under crossed nicols. NSOM and POM observations were carried out at ca. 303 K in air.

3. Results and discussion

3.1. Polarizing NSOM observations

Fig. 2(a) and (b) show a polarizing NSOM image and a shear-force topographic image of a banded spherulite in a HDPE film crystallized isothermally at 373 K for ca. 24 h from the melt, respectively. The brighter parts in the polarizing NSOM image (a) and the topographic image (b) correspond to the higher parts in light intensity and in height, respectively. The extinction ring and cross were observed in the polarizing NSOM image shown in Fig. 2(a). However, a part of the extinction cross in the vibration direction of incident light at the exit of the NSOM aperture was not as dark as that in the direction of the analyzer. This is due to the depolarization effect at the exit of the NSOM aperture. As shown in Fig. 2(b), the center of the spherulites was observed as the highest part in the film surface. There

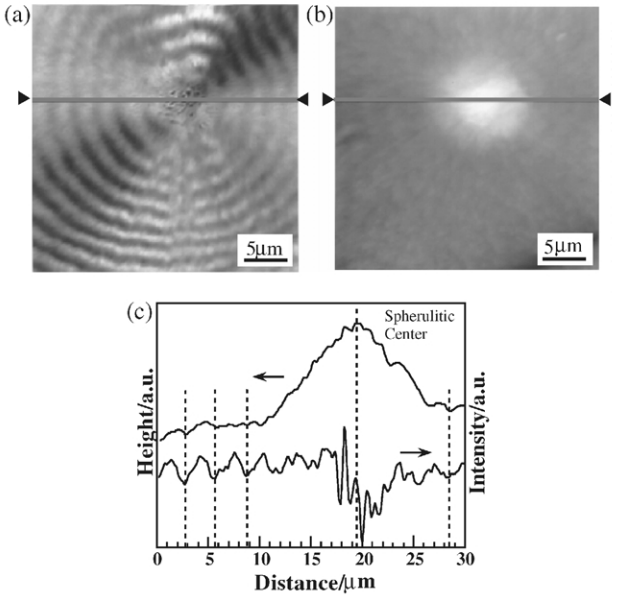

Fig. 2. NSOM images and line profiles of a banded spherulite in a HDPE film prepared by isothermal crystallization at 373 K for ca. 24 h from the melt: (a) polarizing NSOM image; (b) shear-force topographical image; (c) comparison between the light intensity and height profiles along the spherulitic diameter indicated in (a) and (b), respectively.

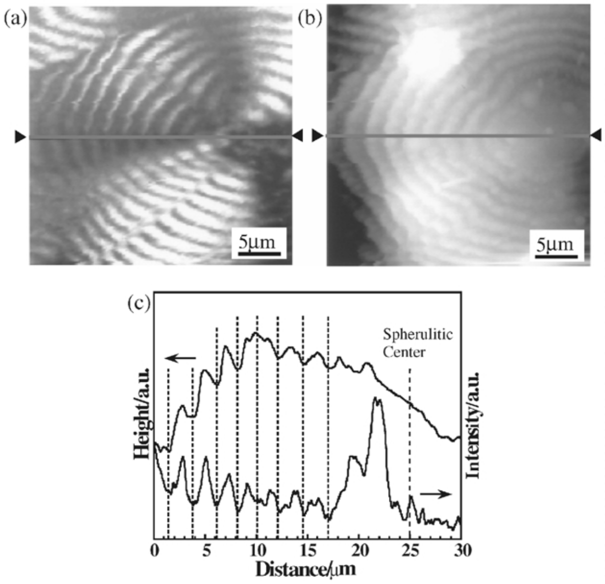

Fig. 3. NSOM images and line profiles of a banded spherulites in an etched HDPE film: (a) polarizing NSOM image; (b) shear-force topographical image; (c) comparison between the light intensity and height profiles along the spherulitic diameter indicated in Fig. 6(a) and (b), respectively. The original banded spherulites were prepared by isothermal crystallization at 373 K for ca. 24 h from the melt.

were small ridges around the spherulitic center. Fig. 2(c) shows comparison between the light intensity profile and the height profile along the spherulitic diameter indicated in Fig. 2(a) and (b), respectively. The light intensity along the spherulitic radius changed corresponding to the height in the corrugation of the film surface. In other words, the band spacing evaluated from the valley-to-valley distance in the height profile was consistent with that of the light intensity profile. This means that the high and low parts in the topographic image corresponded to the bright and dark parts in the NSOM image, respectively. Therefore, polarizing NSOM observation apparently suggests that the crystallographic *c*-axis of the orthorhombic unit cell was parallel and perpendicular to the film surface at the peak and the valley in the surface corrugation of the banded spherulitie, respectively.

In order to investigate crystallographic orientation in the internal of HDPE films, the film surface was etched with permanganic reagent. The original film before etching treatment was prepared by isothermal crystallization at 373 K for ca. 24 h from the melt. Based on the thickness difference between original and etched films evaluated by AFM, the several hundreds nm-thick region was removed from the film surface by etching. Fig. 3 shows a polarizing NSOM image (a) and a shear-force topographic image (b) of a banded spherulite in an etched HDPE film. As shown in Fig. 3(b), the spherulitic center became relatively lower in height. Periodic ridges were developed in the film surface by etching. Fig. 3(c) shows comparison between the height profile and the light intensity profile along the spherulitic diameter indicated in Fig. 3(a) and (b), respectively. There was a good agreement in phase and spacing between the height and intensity profiles. Therefore, it is reasonable to conclude from Figs. 2 and 3 that the periodic corrugation in the surface of the banded spherulite originated from the morphological feature of lamellar twisting in the internal of the films.

3.2. *Crystallization temperature dependence of birefringent and topographic properties*

Fig. 4(a)–(d) show AFM images of banded spherulites in HDPE films crystallized isothermally at $T_c = 373$, 377, 381, and 385 K for 90 h from the melt, respectively. The brighter part in AFM images corresponds to the higher part in surface topography. Periodic ridges were observed as concentric circular patterns in the spherulitic surface. With an increase in crystallization temperature, the regularity of these ridges in the azimuthal direction of the spherulite became lower and the inter-spherulitic boundary became unclear. The spacing of the periodic ridges along the spherulitic radius was evaluated as the band spacing by AFM height measurements. Fig. 5 shows the isothermal crystallization temperature dependence of the band spacing of HDPE spherulites evaluated by AFM, NSOM and POM. At the lower isothermal crystallization temperature around 370 K, polarizing NSOM identified the extinction ring, which was not clearly observed by POM. The band spacing evaluated by AFM and polarizing NSOM increased with an increase in crystallization temperature, which was in good agreement with that evaluated by POM. Also, Fig. 6

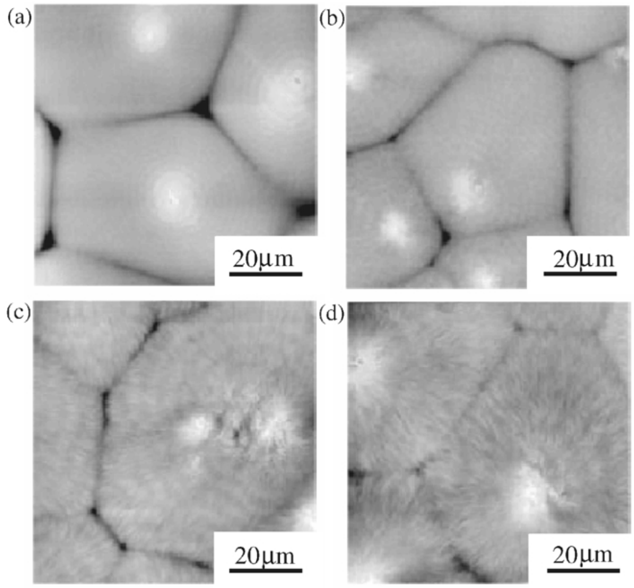

Fig. 4. AFM images of HDPE banded spherulites crystallized isothermally at T_c = (a) 373 K, (b) 377 K, (c) 381 K and (d) 385 K for 90 h from the melt.

shows crystallization temperature dependence of the peak-to-valley height difference in surface corrugations of banded spherulites in HDPE films. It was revealed that the peak-to-valley height difference increased with an increase in isothermal crystallization temperature. These topographic changes in the film surface relate to the lamellar size and the degree of space filling in the region surrounded by twisted lamellae. Supposed that each lamellar crystal continuously twists corresponding to a corrugation of the film surface as shown in Fig. 7, the peak-to-valley height difference in a periodical corrugation changed depending on the width of the lamellar crystal. Therefore, it is reasonably considered from Fig. 6 that the lamellar width increased with increasing isothermal crystallization temperature [16–18]. Since the band spacing and the peak-to-valley height difference drastically changed in value around T_c = ca. 380 K, these topographic changes might imply that spherulitic structure changed from the banding structure to axialitic structure with increasing crystallization temperature [16,17].

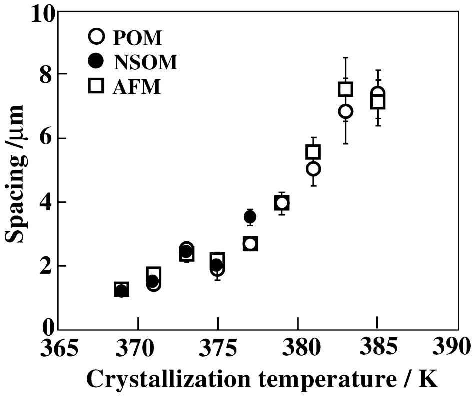

Fig. 5. Isothermal crystallization temperature dependence of the band spacing of HDPE shperulites evaluated by AFM, NSOM and POM.

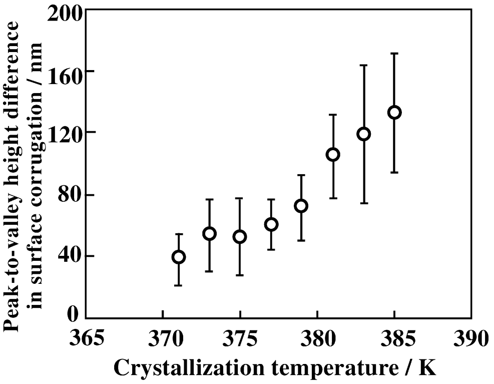

Fig. 6. Isothermal crystallization temperature dependence of the peak-to-valley height difference in surface corrugations of banded spherulites in HDPE films.

Fig. 8(a)–(d) show AFM images of lamellar aggregates in HDPE banded spherulites crystallized isothermally at T_c = 373, 377, 381 and 385 K for 90 h from the melt, respectively. Lath-like or fibrous morphology reflects lamellar aggregation condition in the surface of banded spherulites. As shown in Fig. 2, it was suggested from NSOM data that the crystallographic *c*-axis of the orthorhombic unit cell was parallel to the film surface in the higher part of the spherulitic surface. Therefore, it was reasonable to consider that fibrils observed in the higher part in Fig. 8 corresponded to the edge-on lamellar aggregates. As shown in Fig. 8(a), numerical sheaves of the edge-on lamellar aggregates were cooperatively arranged along the spherulitic radius. With increasing isothermal crystallization temperature, adjacent lamellar aggregates became disordered along the spherulitic radius. Also, the lamellar aggregates became longer along the spherulitic radius and thicker. Fig. 9(a) shows an AFM magnification image of the region inside of a white square in Fig. 8(a). It was directly observed that stacked lamellae exhibited the flat-on and the edge-on orientation in the lower and higher height parts, respectively. The edge of lamellar aggregates was slightly wavy, which suggested that the lamellar edge in the spherulitic surface might be formed with disordered crystals and/or amorphous. The C-bent and the S-bent lamellae were complicatedly stacked as a part of the spherulitic banding

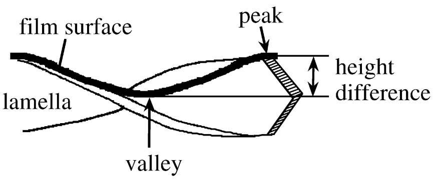

Fig. 7. A simple model explaining the relationship between a continuously twisted lamella and the peak-to-valley height difference in a surface corrugation of a HDPE film.

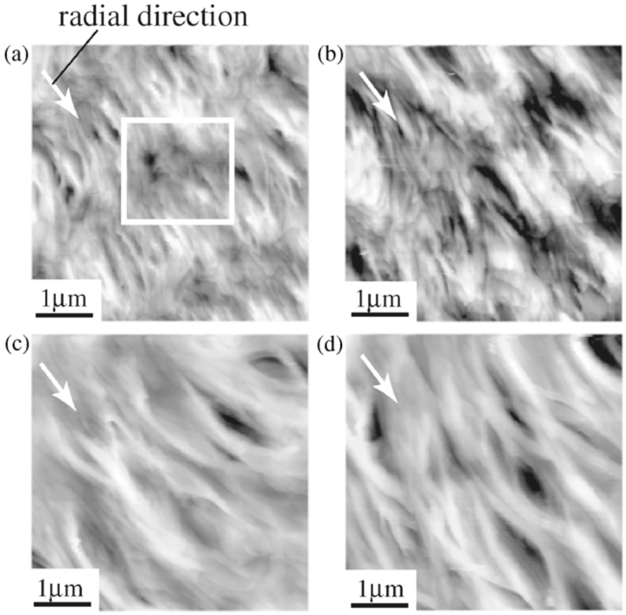

Fig. 8. AFM images of lamellar aggregates in HDPE banded spherulites crystallized isothermally at T_c = (a) 373 K, (b) 377 K, (c) 381 K and (d) 385 K for 90 h from the melt. The region inside of a white square in (a) is magnified in Fig. 9.

[4,7]. As shown in Fig. 9(a) the S-bent lamellae lied in the distance corresponding to a half pitch of the spherulite banding. However, it was still unclear the real length and width of an individual lamella. Fig. 9(b) shows a height profile of the surface of the edge-on lamellar aggregates along a black line in Fig. 9(a). The peak-to-peak distance in the surface corrugation in Fig. 9(b) apparently indicates the distance between the adjacent edge-on lamellae. Fig. 10 shows the isothermal crystallization temperature dependence of the distance between adjacent edge-on lamellae and thickness of an edge-on lamellar aggregate in HDPE banded spherulites evaluated by AFM. With an increase in crystallization temperature from 373 to 385 K, the distance between adjacent edge-on lamellae increased approximately from 25 nm to 45 nm. In addition, thickness of a lamellar aggregate increased approximately from 110 nm to 220 nm. The distance between the adjacent lamellae plotted in Fig. 10 was a little larger than the long-period reported based on small-angle X-ray scattering data of HDPE [16–18]. One explanation for this difference might be that edge-on lamellae in the higher region in the spherulitic surface were slightly tilted from the film normal. Based on Fig. 10, it was suggested that a sheaf of the edge-on lamellae consisted of approximately five major lamellae.

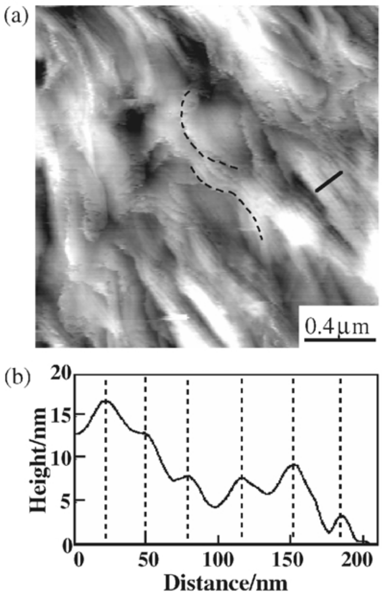

Fig. 9. Lamellar aggregates in a HDPE banded spherulite crystallized isothermally at T_c = 373 K from the melt: (a) AFM magnification image; (b) height profile along a black line indicated in (a). The broken lines indicate the C-bent and the S-bent lamellae as examples.

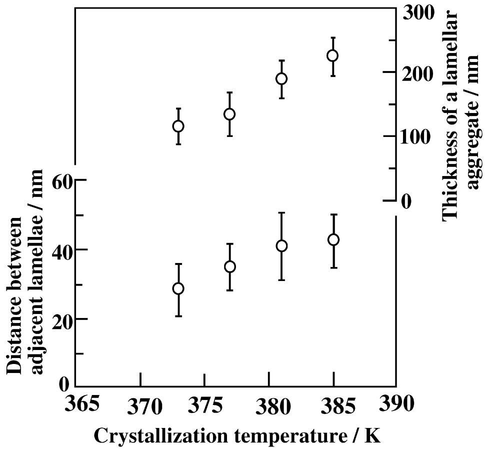

Fig. 10. Isothermal crystallization temperature dependence of the distance between adjacent edge-on lamellae and thickness of an edge-on lamellar aggregate in HDPE banded spherulites evaluated by AFM.

4. Conclusions

The microscopic correlation between the surface topography and local birefringence of banded spherulites in the melt-crystallized HDPE films was revealed by AFM and polarizing NSOM. The height profile of the film surface along the spherulitic radius changed corresponding to the light intensity profile in NSOM. In other words, the high and low parts in the surface corrugation of banded spherulites corresponded to the bright and dark parts in the extinction ring, respectively. The band spacing and the peak-to-valley height difference in the periodic corrugation of the spherulitic surface increased with an increase in isothermal crystallization temperature. It was suggested that the lamellar thickness and width increased with an increase in isothermal crystallization temperature.

AFM observations directly distinguished an individual lamella from the edge-on lamellar aggregates with thickness of several-hundreds nanometers in the higher part of the surface corrugation of banded spherulites. The thickness of a lamellar aggregate and the distance between the adjacent lamellae were evaluated by AFM height measurements.

Acknowledgements

This research was partly supported by Grant-in-Aids for Scientific Research on Priority Areas (A) (#286), Near-field Nano-optics and COE Research (#08CE2005) from the Ministry of Education, Culture, Sports, Science and Technology, Japan.

References

[1] Keller A. J Polym Sci 1955;17:291–308.
[2] Keith HD, Padden Jr. FJ. J Polym Sci 1958;31:415–21.
[3] Keith HD, Padden Jr. FJ. J Polym Sci 1959;39:101–22.
[4] Keith HD, Padden Jr. FJ. J Polym Sci 1959;39:123–59.
[5] Price FP. J Polym Sci 1959;39:139–50.
[6] Keller A. J Polym Sci 1959;39:151–73.
[7] Keith HD, Padden Jr. FJ. Polymer 1984;25:28–42.
[8] Keith HD, Padden Jr. FJ. Macromolecules 1996;29:7776–86.
[9] Bassett DC, Hodge AM. Polymer 1978;19:469–72.
[10] Olley RH, Hodge AM, Bassett DC. J Polym Sci, Polym Phys Ed 1979;17:627–43.
[11] Bassett DC, Hodge AM. Proc R Soc Lond 1981;A377:25–37, see also 39–60, 61–71.
[12] Naylor L, Phillips PJ. J Polym Sci, Polym Phys Ed 1983;21:2011–26.
[13] Bassett DC. Phil Trans R Soc Lond 1994;A348:29–43.
[14] Janimak JJ, Markey L, Stevens GC. Polymer 2001;42:4675–85.
[15] Fujiwara Y. J Appl Phys 1960;4:10–15.
[16] Hoffman JD, Lauritzen JI. J Res Natn Bur Stand A 1961;65A:297–336.
[17] Hoffman JD, Frolen LJ, Ross GS, Lauritzen JI. J Res Natn Bur Stand A 1975;79A:671–99.
[18] Mandelkern L, Posner AS, Diorio AF, Roberts DE. J Appl Phys 1961;32:1509–17.